$Al_xGa_{1-x}As$ nested waveguide heterostructures for continuously phase-matched terahertz difference frequency generation

C. M. Staus,[1] T. F. Kuech,[2] and L. McCaughan[1]*

[1] *Department of Electrical and Computer Engineering, University of Wisconsin-Madison, Madison, WI 53706, USA*
[2] *Department of Chemical and Biological Engineering, University of Wisconsin-Madison, Madison, WI 53706, USA*
**mccaughan@engr.wisc.edu*

Abstract: We previously demonstrated a nested pair of single mode (pump/THz) waveguides which produced guided far-infrared (1.3 THz) light with a record power-normalized conversion efficiency of $1.3x10^{-7}$ W^{-1} by way of continuous phase matched difference frequency generation (DFG) [Opt. Express **16**, 13296 (2008)]. Using the same numerical simulation tools we used to design and model this $LiNbO_3$-based device, we show that a lattice-matched AlGaAs heterostructure, with its significantly lower absorption losses, can produce guided far-infrared light (3.5 THz) with a power-normalized conversion efficiency of 1.3×10^{-5} W^{-1} – some 100 times larger than achieved with the $LiNbO_3$ structure.

OCIS codes: (190.4223) Nonlinear wave mixing; (190.4390) Nonlinear optics, integrated optics; (190.5970) Nonlinear optics, including MQW; (310.6845) Thin film devices and applications.

References and links

1. C. Staus, T. F. Kuech, and L. McCaughan, "Continuously phase-matched terahertz difference frequency generation in an embedded-waveguide structure supporting only fundamental modes," Opt. Express **16**(17), 13296–13303 (2008).
2. J. A. Armstrong, N. Bloembergen, J. Ducuing, and P. S. Pershan, "Interactions between light waves in a nonlinear dielectric," Phys. Rev. **127**(6), 1918–1939 (1962).
3. D. E. Thompson, and P. D. Coleman, "Step tunable far infrared radiation by phase matched mixing in planar dielectric waveguides," IEEE Trans, MTT **22**(12), 995–1000 (1974).
4. Y. Takushima, S. Y. Shin, and Y. C. Chung, "Design of a LiNbO3 ribbon waveguide for efficient difference frequency generation of THz wave in the collinear configuration," Opt. Express **15**(22), 14783–14792 (2007).
5. W. Shi, Y. J. Ding, and P. G. Schunemann, "Coherent terahertz waves based on difference-frequency generation in an annealed zinc-germanium phosphide crystal: improvements on tuning ranges and peak powers," Opt. Commun. **233**(1-3), 183–189 (2004).
6. M. Schall, H. Helm, and S. R. Keiding, "Far infrared properties of electro-optic crystals measured by THz time-domain spectroscopy," Int. J. Infrared Millim. Waves **20**(4), 595–604 (1999).
7. M. R. Brozel, and G. E. Stillman, Properties of Gallium Arsenide, Datareviews Series 16 (The Institution of Electrical Engineers, London, United Kingdom, 1996).
8. H. R. Chandrasekhar, and A. K. Ramdas, "Nonparabolicity of the conduction band and the coupled plasmon-phonon modes in n-GaAs," Phys. Rev. B **21**(4), 1511–1515 (1980).
9. S. Adachi, Properties of Aluminum Gallium Arsenide, Datareviews Series 7 (The Institution of Electrical Engineers, London, United Kingdom, 1996).
10. K. L. Vodopyanov, M. M. Fejer, X. Yu, J. S. Harris, Y. S. Lee, W. C. Hurlbut, V. Kozlov, D. Bliss, and C. Lynch, "Terahertz-wave generation in quasi-phase-matched GaAs," Appl. Phys. Lett. **89**(14), 141119 (2006).
11. C. Lynch, D. F. Bliss, T. Zens, A. Lin, J. S. Harris, P. S. Kuo, and M. M. Fejer, "Growth of mm thick orientation patterned GaAs for IR and THz generation," J. Cryst. Growth **310**(24), 5241–5247 (2008).
12. S. Adachi, "GaAs, AlAs and $Al_xGa_{1-x}As$ material parameters for use in research and device applications," J. Appl. Phys. **58**(3), R1–R29 (1985).
13. T. Tamir, ed., Guided-Wave Optoelectronics (Springer-Verlag, Berlin, Germany, 1990).
14. E. Palik, ed., Handbook of Optical Constants of Solids, (Academic Press, Orlando, FL, (1985).
15. Y. R. Shen, *Nonlinear Infrared Generation*, (Springer-Verlag, Berlin Heidelberg, 1977).
16. J. S. Blakemore, "Mid-infrared dispersion of the refractive index of and reflectivity for GaAs," J. Appl. Phys. **62**(11), 4528 (1987).
17. D. N. Nikogosyan, Properties of Optical and Laser-related Materials, (Wiley, Chichester, 1997), p. 333.

#120268 - $15.00 USD Received 19 Nov 2009; revised 9 Jan 2010; accepted 11 Jan 2010; published 21 Jan 2010

Introduction

Ultra-high resolution (i.e., < 1 MHz) linear and nonlinear spectroscopy above one THz (i.e., far infrared) provides new windows through which to view both rotational and coupling resonances of small molecules. These rotational and vibrational spectral features also serve as probes of the internal molecular environment of macromolecules containing these simpler molecular subunits. Because of the limited resolution of THz spectrometers, the source itself must be spectrally pure. Difference frequency generation (DFG), pumped by narrow-band CW optical sources, provides one of the very few methods of producing continuously tunable room temperature radiation at and above one THz with sub-MHz linewidth. That said, to achieve reasonable output powers (> 1 μW) requires significantly larger conversion efficiency than has been demonstrated in bulk materials.

Larger DFG conversion efficiency requires strong confinement of the two optical pumps and THz product, good overlap of the 3 fields over a long interaction length, and maintenance of the spatial synchrony between the induced polarization wave and the electromagnetic wave product (i.e., phase matching). Under the proper conditions, optical waveguiding can improve both the overlap and the confinement-length product above diffractive free space conditions. For collinear guided wave DFG, $\omega_3 = \omega_1 - \omega_2$, phase matching can be expressed as $\Delta\beta = \beta_1 - \beta_2 - \beta_3 = 0$, where $\beta_{1,2}$ and β_3 are the mode propagation constants for the pumps and THz, respectively. Continuously phase matched difference frequency generation of THz light (approximately 40% more efficient than first order quasi-phase matching [2]) has been demonstrated using inter-modal dispersion in waveguides [3,4], but the efficiency gained in continuous phase matching is offset by a poor pump/product mode overlap.

Material constraints usually preclude fabricating a single waveguide which provides strong confinement, good modal overlap of pumps and product, and continuous phase matching. Recently, we demonstrated by numerical simulation, and confirmed by experiment, that a pair of single mode waveguides, one for the two optical pumps (~1550 nm) embedded within the THz-bearing guide (231 μm, 1.3 THz), can provide the necessary degrees of freedom to achieve continuous phase matching [1]. The $LiNbO_3$-based hybrid waveguide configuration exhibited a power normalized DFG conversion efficiency $\eta_p = P_3/P_1P_2 = 1.3 \times 10^{-7}$ W^{-1} at 1.3 THz, some 23-fold large than the best previously reported results [5]. Continuous phase matching arises from the fact that the propagation constant of the surrounding THz waveguide (β_3) can be manipulated nearly independent of the waveguide properties of the smaller pump guides (specifically β_1 and β_2).

While $LiNbO_3$ has a large optical nonlinearity for THz DFG (175 pm/V), its absorption coefficient is also large and increases rapidly with increasing frequency, e.g., 2α(1.5 THz)~32 $cm^{-1}$and 2α(3.5 THz) ~1600 cm^{-1} [6], quenching the THz field and thus limiting the useful tuning range to ~2 THz (see Fig. 2(b) of [1]). (Al)GaAs, with its significantly lower loss over a large range of the far infrared, 2α(1.5 THz)~1.1 cm^{-1} and 2α(3.5 THz) ~2.2 cm^{-1} [7–9], and the ability to fabricate index guided structures heteroepitaxially, should be a superior nonlinear material, if a continuous phase matching structure can be produced. THz generation has previously been demonstrated in bulk quasi-phase matched GaAs [10,11]. In addition to its relatively large 2nd order nonlinearity and low loss at both the THz and near-infrared wavelengths, (Al)GaAs exhibits a small refractive index difference between the THz and near-infrared. We demonstrate here that, by taking advantage of this latter attribute and the ability to fabricate epitaxially grown heterostructure waveguides, an AlGaAs pump waveguide can be embedded in a THz waveguide, providing strong mode confinement, low modal loss, and continuous phase matching between the pumps and THz product. We note that while the optical properties of $Al_xGa_{1-x}As$ are well known as a function of Al fraction x in the near IR, very few measurements of its optical characteristics have been made in the THz (λ<300 μm) for $x \neq 1$. Where possible, we have used [9] to extrapolate the values of the optical constants of $Al_xGa_{1-x}As$ in the THz from those of GaAs.

#120268 - $15.00 USD Received 19 Nov 2009; revised 9 Jan 2010; accepted 11 Jan 2010; published 21 Jan 2010

AlGaAs embedded waveguide structure

The proposed AlGaAs embedded waveguide structure for THz DFG is shown in Fig. 1. In order to take advantage of the ready availability of fiber-based optical circuit elements (pigtailed laser diodes, fiber amplifiers, polarization controllers, etc.), the pump rib waveguide was designed for single mode operation and reasonably good mode overlap with standard 1550 nm single mode telecommunications optical fiber. Assuming a minimum pump wavelength of λ_1 = 1.535 μm, two-photon absorption, $2\hbar\omega_1$ = 1.616 eV, can be avoided by using $Al_xGa_{1-x}As$ with an aluminum concentration greater than 16% (i.e. $E_g[eV] = 1.424 + 1.24x \geq 2\hbar\omega_1$ [12,13], where E_g is the bandgap of AlGaAs). The two pumps are therefore confined to an $Al_{0.18}Ga_{0.82}As/Al_{0.16}Ga_{0.84}As/Al_{0.18}Ga_{0.82}As$ fundamental mode rib waveguide. The THz light, generated through the DFG process, is guided by a larger fundamental mode rib air/AlGaAs/Si waveguide, whose core consists of the three inner AlGaAs layers.

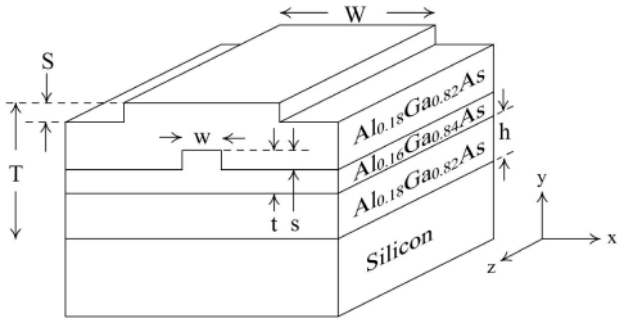

Fig. 1. Diagram of the AlGaAs nested waveguide structure. The pump rib waveguide is defined by the AlGaAs layers and dimensions s, t, and w. The THz waveguide is defined by the pump layers and the rib dimensions S, T, and W.

The modal properties of the pump waveguide are determined by the inner waveguide geometry defined by t, s, and w in Fig. 1, as well as by the composition of the AlGaAs heterostructure. The refractive index of $Al_xGa_{1-x}As$ as a function aluminum concentration and wavelength can be described by $n(\lambda, x) = n_{GaAs}(\lambda) - 0.45x$ for λ > 1.1 μm, where $n_{GaAs}(\lambda)$ is the refractive index of GaAs [13]. The core layer has an aluminum concentration that is 2% smaller than surrounding cladding (18%), which corresponds to a positive refractive index difference of 0.009 for λ_1 =1.535 μm. The 2% change in aluminum concentration is chosen to represent realistic capabilities of Al concentration control in a chemical vapor deposition (CVD) growth system. Given Δn = 0.009, the pump rib waveguide geometry was designed for a fundamental TE mode (E-field ‖ x in Fig. 1 and Fig. 2) with a large transverse mode profile at 1.535 μm (Fig. 2). The FWHMs of the rib mode along x and y are 7.5 μm and 3.5 μm, respectively, which are smaller than the ~9 μm FWHM of standard 1.5 μm optical fiber.

#120268 - $15.00 USD Received 19 Nov 2009; revised 9 Jan 2010; accepted 11 Jan 2010; published 21 Jan 2010

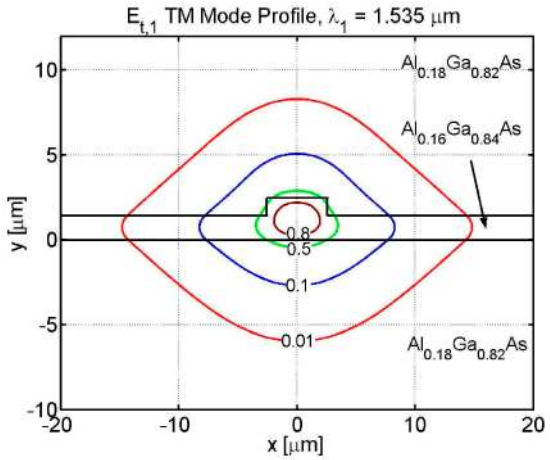

Fig. 2. TM (E-field ‖ y) fundamental mode of the inner rib waveguide at a pump wavelength of λ_1 = 1.535 μm. Rib dimension are t = 2.5 μm, s = 1 μm, and w = 5 μm. The peak electric field amplitude is normalized to 1.

The overlap of the pump rib waveguide mode in Fig. 2 with a standard fiber mode at 1.535 μm (V parameter = 2.4, core radius = 4.5 μm) was calculated to be 0.78. Further improvement could be made by increasing the pump mode size along y by reducing the difference in aluminum concentration (and therefore reducing Δn) between the AlGaAs core and cladding layers.

The THz waveguide is formed by the whole of the AlGaAs heterostructure, clad with the silicon substrate on one side and air on the other. Mode field calculations (like those carried out in Fig. 2) show that the pump modes are not influenced by the THz waveguide geometry (dimensions T, S, and W in Fig. 1), or by the choice of THz cladding materials (Si and air, in this case) when the $Al_{0.18}Ga_{0.82}As$ cladding layers of the pump rib structure are greater than ~7 μm, The choice of cladding materials and geometry of the THz waveguide can therefore be made independent of the pump waveguide for single mode operation, good mode confinement, and phase matching to the near-IR pumps. Silicon was selected as the lower cladding layer because of its low absorption (2α ~0.4 cm^{-1} at λ = 83.3 μm) and refractive index value (n_{Si} ~3.4 at λ = 83.3 μm) [14], which is only slightly smaller than that of GaAs in the THz (n_{GaAs} ~3.6 and 2α ~2.2 cm^{-1} at λ = 83.3 μm) [7,8]. As a consequence, the THz waveguide can support a single fundamental mode whose propagation constant β_3 satisfies the phase matching condition, $\Delta\beta = \beta_1 - \beta_2 - \beta_3 = 0$. Given silicon and air as the cladding layers, the THz propagation constant is now determined by the total AlGaAs thickness T, shoulder height S, and the rib width W.

Phase matching analysis

GaAs has the point group symmetry $\bar{4}3m$ for which the nonzero nonlinear coefficients are $d_{14} = d_{25} = d_{36}$. In the analysis that follows, the crystal orientation of the AlGaAs is assumed to be (100) ([100] parallel to the y – axis of Fig. 1.). In this case, TE polarized pumps propagating along the [011] or $[0\bar{1}1]$ crystal directions (which would be oriented parallel to the z-axis in Fig. 1) generate a TM polarized THz field (E-field along y in Fig. 1.) It should be noted that the (111) orientation has a larger effective nonlinearity $d_{eff} = \frac{2}{\sqrt{3}} d_{14}$, compared to $d_{eff} = d_{14}$ for the (100) orientation [15]. In the (111) case, the pumps and THz product are TM polarized and the waveguides can be oriented along any direction in the x-z plane in Fig. 1. The (100) orientation is considered here because it is a widely used substrate for AlGaAs CVD growth.

#120268 - $15.00 USD Received 19 Nov 2009; revised 9 Jan 2010; accepted 11 Jan 2010; published 21 Jan 2010

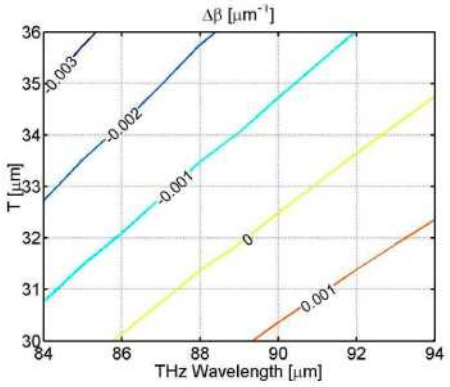

Fig. 3. Phase mismatch Δβ for the (100) AlGaAs nested waveguidestructure. S = 15 μm and W = 50 μm.

Figure 3 is a contour plot of the phase mismatch $\Delta\beta = \beta_1 - \beta_2 - \beta_3$ as a function of THz wavelength and total AlGaAs thickness T for the (100) AlGaAs crystal orientation. The THz rib shoulder height S and width W are fixed at 15 μm and 50 μm, respectively, and the wavelength of the higher frequency pump λ_1 was fixed at 1.535 μm. The pump waveguide geometry used in the simulation is identical to that given in the caption of Fig. 2. The mode propagation constants for the two pumps and THz were calculated using a 2-D beam propagation software. Refractive index data for $Al_xGa_{1-x}As$ in the near-IR and for silicon in the THz were taken from references [14,16]. All of the AlGaAs layers were assumed to have the same refractive index and absorption values as GaAs in the THz [7–9]. (The THz refractive index measurements in references [7,8] were taken from a GaAs sample with an electron density of 1.8 x 10^{16} cm^{-3}.). The material absorption coefficients of GaAs and silicon were included in the THz mode calculations. In the (Al)GaAs case, the absorption values were a function of wavelength, ranging from 2.2 cm^{-1} at 80 μm to 1.4 cm^{-1} at 94 μm [7–9]. The imaginary part of the refractive index for Si was assumed to be constant from 80 to 94 μm, with a value of $K=\lambda\alpha/2\pi=2.9 \times 10^{-4}$ [14]. The THz rib waveguide was found to be single mode for all combinations of dimension T and the THz wavelength shown in Fig. 3. By choosing the appropriate thickness T, the embedded waveguide structure can be tailored to a specific THz output frequency.

THz output power and conversion efficiency

The THz output power of the AlGaAs nested waveguide was calculated for T = 30 μm in Fig. 3 using from [1]:

$$P_3(L) = \frac{\omega_3^2 \varepsilon_o^2 |\Gamma|^2}{4(\alpha_3^2 + \Delta\beta^2)|\Omega_3|^2} P_1 P_2 \left(e^{-2\alpha_3 L} - 2e^{-\alpha_3 L}\cos(\Delta\beta L) + 1\right) = \eta_p P_1 P_2. \qquad (1)$$

For comparison, the device length and pump powers were chosen to be identical to the values used in the $LiNbO_3$ based structure [1], L = 11 mm, $P_1 = P_2$ = 760 mW. The overlap integral in Eq. (1) is defined as

$$\Gamma = \iint d_{eff} E_{t,1} E_{t,2}^* E_{t,3} dxdy, \qquad (2)$$

where $E_{t,,m}$ and $H_{t,m}$ (m = 1,2,3) are the fundamental transverse electric and magnetic mode profiles at ω_m and are normalized according to

$$\tfrac{1}{2}\iint \mathrm{Re}\left[\left(\mathbf{E}_{t,m} \times \mathbf{H}_{t,m}\right)\right] \cdot \hat{z}\, dxdy = 1\,\mathrm{W}, \mathbf{H}_{t,m} = i/(\omega_m \mu_o)\nabla \times \mathbf{E}_{t,m}. \qquad (3)$$

The orthogonality constant for the lossy THz mode in Eq. (1) is given by

#120268 - $15.00 USD Received 19 Nov 2009; revised 9 Jan 2010; accepted 11 Jan 2010; published 21 Jan 2010

$$\Omega_3 = 1/2 \iint \left(\mathbf{E}_{t,3} \times \mathbf{H}_{t,3} \right) \cdot \hat{z}\, dxdy. \quad (4)$$

The amplitude absorption coefficient for the THz mode is represented by α_3. Here we have used the d_{eff} value associated with that of GaAs, since to the best of our knowledge, values for $Al_xGa_{1-x}As$ have yet to be determined for THz DFG. The effective nonlinearity for the (100) AlGaAs embedded waveguide structure (TE polarized pumps and TM THz output) is therefore taken to be $d_{eff} = d_{14} = 47$ pm/V, where d_{14} is the nonlinear coefficient of GaAs [10,17]. Equations (1-4) assume that the two pump powers are undepleted and that the pump waveguide losses are zero.

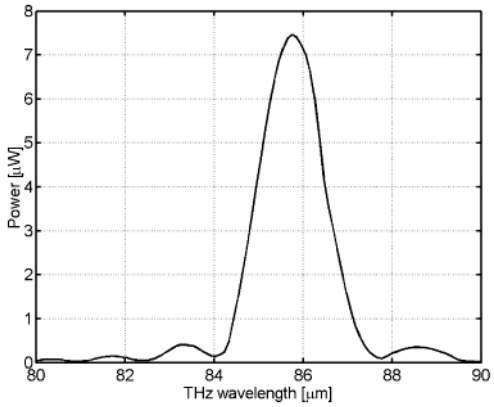

Fig. 4. Calculated THz output power P_3 for the (100) based AlGaAs embedded waveguide structure. The device length and pumps powers were L = 11 mm and $P_1 = P_2$ = 760 mW, respectively.

The output power vs. THz wavelength is shown in Fig. 4, with λ_1 fixed at 1.535 μm. A waveguide offset of h = 10 μm (see Fig. 1) provides optimal pump/THz mode overlap. The maximum output power of 7.5 μW occurs at a wavelength of 85.75 μm (3.5 THz). The DFG power-normalized conversion efficiency, given by $\eta_p = P_3/(P_1P_2)$, for the (100) AlGaAs structure is $\eta_p = 1.3 \times 10^{-5}$ W^{-1}. This result is ~100 times larger than the experimental result for the $LiNbO_3$ embedded waveguide structure [1], and ~2000 fold larger than the best demonstration to date in bulk (estimated from data in [5] to be ~5.6×10^{-9} W^{-1}). Unlike the $LiNbO_3$ result of [1], which requires weak THz mode confinement to achieve phase matching, the small index difference in AlGaAs between pumps and product permits phase matching while maintaining strong THz confinement to the AlGaAs structure. Conversion efficiency also benefits from low waveguide losses in the THz. Figure 5 is the electric field profile of the phase matched THz mode (λ_3 = 85.75 μm). The THz mode is reasonably well confined to the AlGaAs core layers with a low mode absorption coefficient of $2\alpha_3$= 1.4 cm^{-1}.

#120268 - $15.00 USD Received 19 Nov 2009; revised 9 Jan 2010; accepted 11 Jan 2010; published 21 Jan 2010

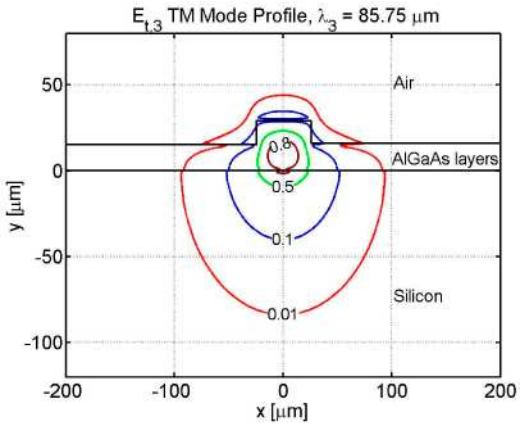

Fig. 5. TM (E-field ‖ y) fundamental mode of the THz rib waveguide at λ_3 = 85.75 μm (3.5 THz). The rib dimensions are T = 30 μm, S = 15 μm, and W = 50 μm (see Fig. 1). The power absorption coefficient is $2\alpha_3$ = 1.4 cm^{-1}. The peak electric field amplitude is normalized to one.

We find that phase matching results for the (111) orientation are essentially the same for the (100). The difference in the pump propagation constants between TE and TM polarizations in the IR waveguide is negligible; as a result the phase mismatch plot for (111) is identical to (100) shown in Fig. 4. The maximum output power occurs at the same wavelength of 85.7 μm, but the output power and normalized conversion efficiency are 4/3 times larger (P_3 = 10 μW; η_p=1.8 x 10^{-5} W^{-1}) because of the higher effective nonlinearity for the (111) orientation.

Conclusion

We have shown by numerical simulation that an AlGaAs single mode 1550 nm rib waveguide embedded within a composite (Si/AlGaAs/air) single mode far-infrared (THz) waveguide can produce continuously phase matched light by difference frequency generation at ~3.5 THz with record high efficiency. In particular, the calculated normalized power conversion efficiency η_p=1.3 x 10^{-5} W^{-1} at 3.5 THz for (100) oriented AlGaAs is some 100 times larger than that achieved with a similar $LiNbO_3$ structure [1], and ~2000 fold larger than the best demonstration to date in bulk (estimated from data in [5] to be ~5.6 x 10^{-9} W^{-1}). We note finally that the embedded waveguides of the type depicted in Fig. 1 can be fabricated using standard semiconductor growth and processing techniques, such as chemical vapor deposition (CVD), photolithography, and wet etching. While the heterostructure would be grown on a GaAs substrate, InGaP or AlAs etch stop layers can be incorporated in the lattice-matched structure to facilitate the substrate removal and the transfer of the AlGaAs heterostructure to the silicon platform. Such processing can utilize current wafer bonding techniques and tools.

Acknowledgements

The authors acknowledge the support of AFOSR and the NSF Division of Material Research (DMR-0505775).

#120268 - $15.00 USD Received 19 Nov 2009; revised 9 Jan 2010; accepted 11 Jan 2010; published 21 Jan 2010